Journal of Ceramic Processing Research. Vol. 8, No. 5, pp. 336~340 (2007)

J O U R N A L O F
Ceramic Processing Research

Fabrication and characterization of ethylene-vinyl acetate copolymer/Al_2O_3 nanocomposites

Bo Jin[a,b], Wanxi Zhang[a], Guangping Sun[a,*] and Hal-Bon Gu[b]

[a]*College of Materials Science and Engineering, Jilin University, Changchun 130025, China*
[b]*Department of Electrical Engineering, Chonnam National University, Gwangju 500-757, Korea*

Ethylene-vinyl acetate (EVA)/Al_2O_3 nanocomposites were prepared by means of a "one-pot" process. The structures and morphologies of EVA/Al_2O_3 nanocomposites were characterized by field emission scanning electron microscopy (FESEM), Fourier transform infrared spectroscopy (FT-IR) and scanning electron microscopy (SEM). The mechanical and rheological properties of EVA/Al_2O_3 nanocomposite materials were investigated. FESEM results indicate that Al_2O_3 nanoparticles with a particle of about 20 nm are homogeneously dispersed in the EVA matrix. SEM studies show that EVA/Al_2O_3 nanocomposites transform from brittleness to toughness when ruptured. FT-IR results demonstrate that Al_2O_3 nanoparticles link with EVA through a chemical bond. Compared to that of the pure EVA, the tensile strength and elongation at fracture of EVA/Al_2O_3 nanocomposite material with 1.5% Al_2O_3 fillers increase by 25.4% and 12.1%, respectively. The apparent viscosity of EVA/Al_2O_3 nanocomposite melts is lower than that of the pure EVA, which effectively improves the process fluidity of the EVA/Al_2O_3 nanocomposites.

Key words: EVA, Al_2O_3, Nanocomposite, Tensile strength, Apparent viscosity.

Introduction

In recent years, polymeric-inorganic nanocomposites have aroused people's extensive attention [1-8]. These nanocomposites are where nanoparticles are homogeneously dispersed in the polymer matrix, and these nanoparticles include SiO_2, Al_2O_3, TiO_2, CdSe, montmorillonite, etc. These nanoparticles have a particularly small size effect, quantum size and quantum tunnel effects, surface and volume effects, and their appearance provides a new method for polymeric materials to have excellent performance [9-14]. Al_2O_3 possesses favorable physical and chemical properties such as high strength, hardness, elastic modulus and excellent resistance to thermal and chemical environments. However, its applications are somewhat limited because of poor toughness and inferior thermal resistance [15]. Recently some researchers have studied the intercalated nanocomposites in which EVA is used as the polymer matrix [16-19]. EVA possesses excellent flexibility, impact resilience, optical properties, low temperature-resistance, and is widely used in making packing film and electrical cable sheathing. Tang et al. [16] demonstrated that the heat release rate (HRR) of EVA/montmorillonite nanocomposite was 40% lower than that of pure EVA. Qiu et al. [17, 18] revealed that the limit oxygen index (LOI) of EVA/$Mg(OH)_2$ nanocomposite was 59.6% higher than that of EVA/$Mg(OH)_2$ microcomposite. Tian et al. [19] indicated that compared to that of pure EVA, the tensile strength and tear strength of EVA/montmorillonite nanocomposite increased by 10.8% and 11.6%, respectively.

In this study, EVA/Al_2O_3 nanocomposites were prepared by means of a "one-pot" process, the structures and morphologies of EVA/Al_2O_3 nanocomposites were characterized, and the mechanical and rheological properties of EVA/Al_2O_3 nanocomposite materials were analyzed.

Experimental

Ethylene-vinyl acetate copolymer (EVA, containing 15% vinyl acetate) was purchased from Tosoh Corporation, Japan. Al_2O_3 with a particle of about 10 nm was supplied by the key laboratory of automobile materials in Ministry of Education, Jilin University, China. YGO-1203 vinyltriethoxysilane coupling agent (CH_2=CHSi(OC_2H_5)$_3$) was obtained from the Harbin research institute of the chemical industry, Heilongjiang Province, China. Pure analytical grade olefin and ethanol were used.

EVA, vinyltriethoxysilane coupling agent, olefin and Al_2O_3 nanoparticles were premixed in the appropriate proportion at 60 °C. The mixtures were subsequently put into a twin-roll mill, and melt-mixed for 10 minutes. Eventually, the resulting samples were taken out. The samples were melt-mixed once again for 10 minutes, and ultimately hot-pressed into sheets of 2 mm thick-

*Corresponding author:
Tel : +86-431-5095170
E-mail: sungp@jlu.edu.cn

ness under 12 MPa for 5 minutes at 150 °C. The temperature of the mill was maintained at 110 °C, and the rotation speed was retained at 100 rpm.

The particle size and the dispersion of Al_2O_3 nanoparticles were imaged using a XL30 field emission scanning electron microscopy (Micrion/FEI/Philips, America) at an acceleration voltage of 20 kV and exposure time of 40 s. The sample structures were analyzed using a 360 Fourier transform infrared spectroscopy (NICOLET, America). The tensile strength and elongation at fracture of samples were examined using a WSM-5K omnipotence mechanical testing machine at a strain rate of 50 mm/minute, and the average value of five samples was taken with a standard deviation of less than 6%. The morphologies of ruptured surfaces of samples were observed using a LINK-ISIS JSM5310 scanning electron microscopy (OXFORD, United Kingdom) at an acceleration voltage of 15 kV and exposure time of 40 s. The rheological properties of samples were tested at 170 °C using a XLY-capillary rheometer with an aspect ratio of 40/1.

Results and Discussion

Morphological analysis

The FESEM pattern of an EVA/Al_2O_3 nanocomposite material with 1.5% Al_2O_3 fillers is shown in Fig. 1. It is observed that Al_2O_3 nanoparticles are homogeneously dispersed in the EVA matrix. This implies that no agglomeration of Al_2O_3 nanoparticles exits in the EVA matrix. The particle size of Al_2O_3 nanoparticles was about 20 nm. Al_2O_3 nanoparticles have a small size, high specific surface area, Lewis-acid character, and intense surface activity. Al_2O_3 nanoparticles achieve a nanometer scale dispersion by means of a "one-pot" process, which further enhances the properties of these nanocomposites.

The SEM pattern of a fractured surface of pure EVA is shown in Fig. 2. SEM studies indicate that the fractured surface of pure EVA is flat and smooth, displays a regular layered structure perpendicular to the tensile direction, the matrix in the inner necks ruptures, and pure EVA possesses the characteristics of brittleness fracture.

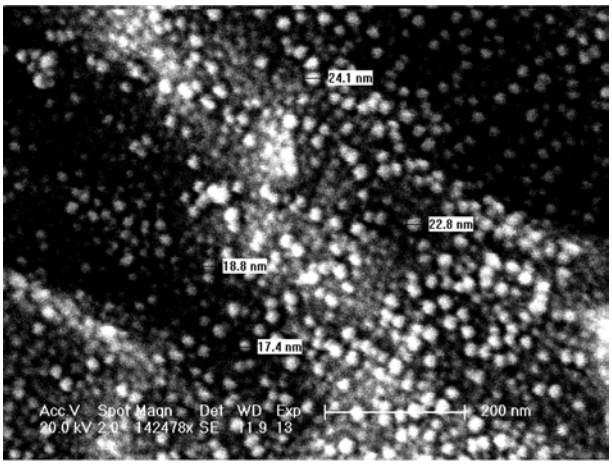

Fig. 1. FESEM pattern of EVA/Al_2O_3 nanocomposite material with 1.5% Al_2O_3 fillers.

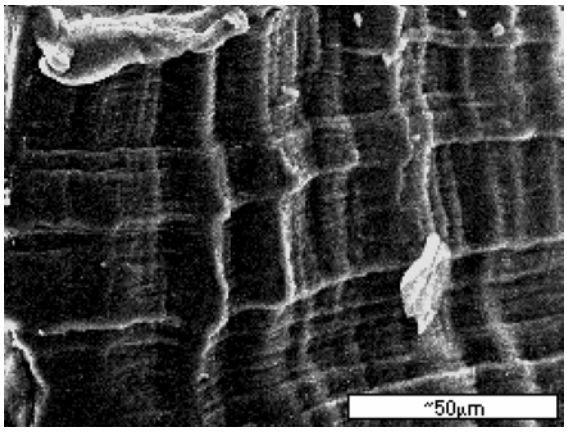

Fig. 2. SEM pattern of a fractured surface of pure EVA.

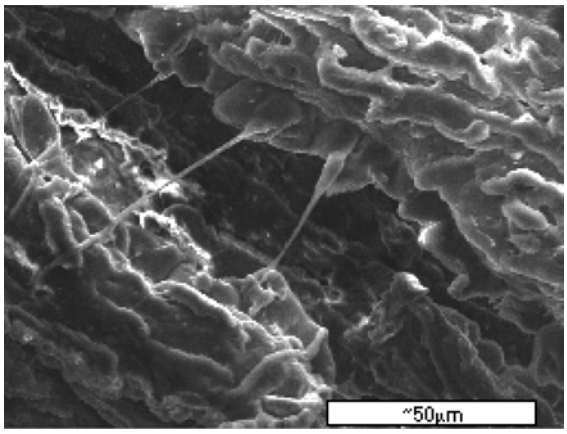

Fig. 3. SEM pattern of a fractured surface of the EVA/Al_2O_3 nanocomposite material with 1.5% Al_2O_3 fillers.

The SEM pattern of a fractured surface of EVA/Al_2O_3 nanocomposite material with 1.5% Al_2O_3 fillers is shown in Fig. 3. SEM studies indicate that the fractured surface of the nanocomposite is rugged, possesses obvious fiber-like threads, and reveals the characteristics of more ductile fracture. The net structures and quite regular cracks indicate that the tensile fracture does not occur at the boundaries of the Al_2O_3 nanoparticles, and gives the enhanced toughness effect.

Structural analysis

An FT-IR pattern of Al_2O_3 nanoparticles is shown in Fig. 4. The absorption peaks at 3430 and 1635 cm^{-1} are ascribed to the stretching vibration and distortion vibration of the hydroxyl (O-H) group, respectively. This clearly indicates that many O-H groups are on the surface of Al_2O_3 nanoparticles, this is mainly due to the intense absorption effect of Al_2O_3 nanoparticles.

The FT-IR patterns of the pure EVA and the EVA/Al_2O_3 nanocomposite with 1.5% Al_2O_3 fillers are shown

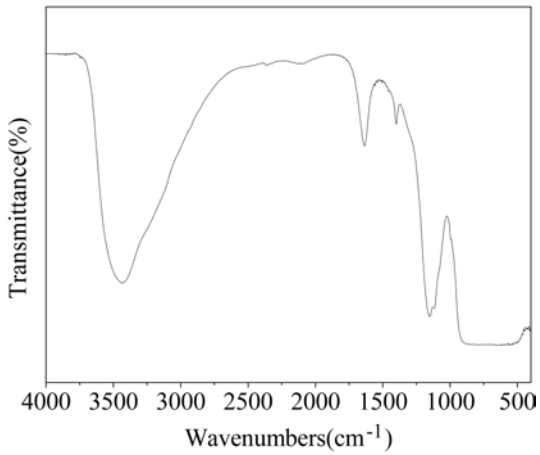

Fig. 4. FT-IR pattern of Al_2O_3 nanoparticles.

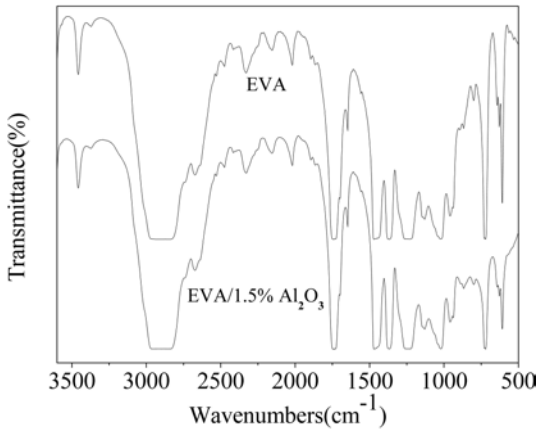

Fig. 5. FT-IR patterns of the pure EVA and the EVA/Al_2O_3 nanocomposites.

in Fig. 5. It is observed that a Si-C absorption peak appears at 868 cm^{-1}, and a C=C absorption peak of the vinyltriethoxysilane coupling agent does not appear. This clearly indicates that the vinyltriethoxysilane coupling agent chemically cross-links with the EVA. It is noted that O-H absorption peaks do not appear at 3430 and 1635 cm^{-1} when Al_2O_3 nanoparticles are present in the EVA matrix. This clearly reveals that the vinyltriethoxysilane coupling agent reacts with the hydroxyl groups. The above results demonstrate that under the effect of the bipolar group of vinyltriethoxysilane coupling agent, a definite chemical bond structure emerges between the active end of the EVA and the O-H group on the surface of Al_2O_3 nanoparticles. The reaction processes of EVA matrix and Al_2O_3 nanoparticles are as follows:

(1) Vinyltriethoxysilane coupling agent hydrolyzes into silanol in air.

$$CH_2{=}CHSi(OC_2H_5)_3 \rightarrow CH_2{=}CHSi(OH)_3$$

(2) The silanol reacts with O-H on the surface of Al_2O_3 nanoparticles, and with the active end of EVA to create the cross-linked copolymer.

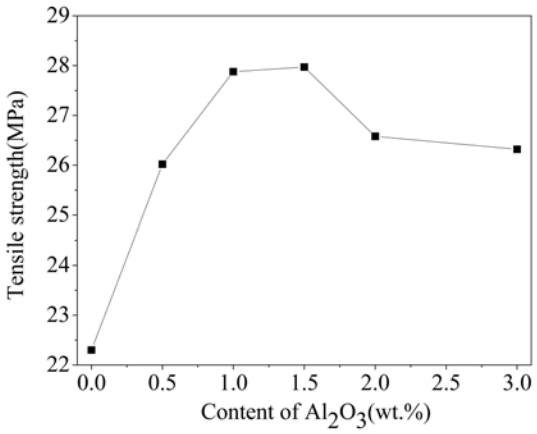

Fig. 6. Influence of Al_2O_3 content on the tensile strength of EVA/Al_2O_3 nanocomposites.

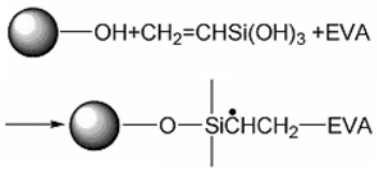

Mechanical properties

The influence of the Al_2O_3 content on the tensile strength of EVA/Al_2O_3 nanocomposites is shown in Fig. 6. The tensile strength of the pure EVA is 22.30 MPa, and the tensile strength of the EVA/Al_2O_3 nanocomposite with 1.5% Al_2O_3 fillers is 27.97 MPa, that is it increases by 25.4%. It is observed that the nanocomposites exhibit a trend with increasing content of Al_2O_3. This clearly indicates that the vinyltriethoxysilane coupling agent has improved the compatibility between the EVA and Al_2O_3, and results in an increase in tensile strength. However, at a higher content of Al_2O_3, i.e. more than 1.5% the tensile strength starts to decrease. The sharp drop in tensile strength at a higher concentration of Al_2O_3 may be due to the agglomeration of Al_2O_3 nanoparticles.

The influence of Al_2O_3 content on the elongation at

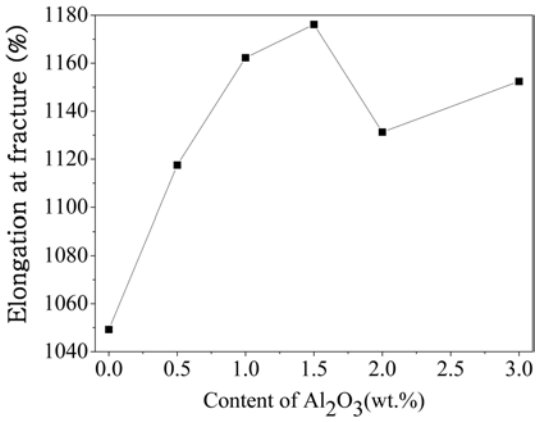

Fig. 7. Influence of Al_2O_3 content on the elongation at fracture of EVA/Al_2O_3 nanocomposites.

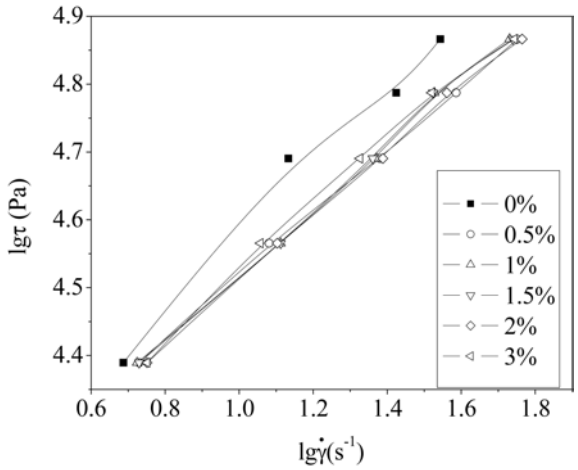

Fig. 8. Influence of the shear rate on the shear stress of EVA/Al_2O_3 nanocomposites at 170 °C.

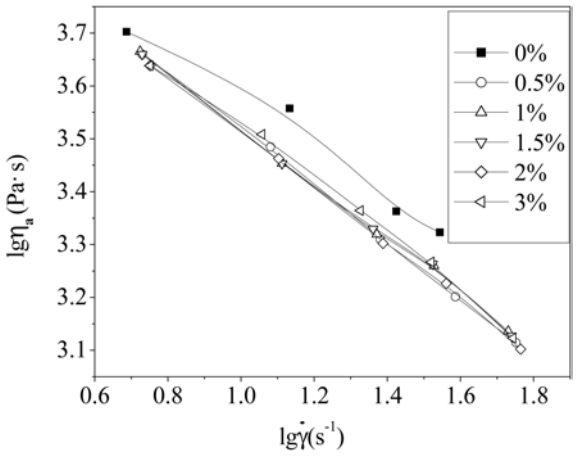

Fig. 9. Influence of the shear rate on the apparent viscosity of the EVA/Al_2O_3 nanocomposites at 170 °C.

fracture of EVA/Al_2O_3 nanocomposites is shown in Fig. 7. The elongation at fracture of the pure EVA is 1050.00%, and the elongation at fracture of the EVA/Al_2O_3 nanocomposite with 1.5% Al_2O_3 fillers is the highest, that is, 1176.17%, i.e. it increases by 12.1%.

From the above tests, it is shown that the mechanical properties of EVA/Al_2O_3 nanocomposites are superior to that of the pure EVA.

Rheological properties

The influence of the shear rate on the shear stress of EVA/Al_2O_3 nanocomposites at 170 °C is shown in Fig. 8. It is observed that the shear flow of low Al_2O_3-filled nanocomposites meets the relation of a power law in principle, namely it can be expressed by $\tau = K^n$, where τ is the shear stress; K is the consistency coefficient; is the shear rate; and n is the rheological index. The rheological indices of EVA/Al_2O_3 nanocomposite melts are shown in Table 1. It is noted that the rheological indices of the EVA/Al_2O_3 nanocomposites are all less than 1, the rheological index of the EVA/Al_2O_3 nanocomposite with 1.5% Al_2O_3 fillers is the lowest, that is, 0.47, and the nanocomposites still exhibit the pseudoplastic flow.

The influence of the shear rate on the apparent viscosity of EVA/Al_2O_3 nanocomposites at 170 °C is shown in Fig. 9. It is seen that the apparent viscosity of the EVA/Al_2O_3 nanocomposites decrease along with an increase of the shear rate. Compared to that of the pure EVA, the flow curves of the EVA/Al_2O_3 nanocomposites obviously shift downwards. This indicates that the EVA/Al_2O_3 nanocomposite melts present pseudoplastic flow characteristics of shear thinning, and the apparent viscosity of EVA/Al_2O_3 nanocomposite melts is lower than that of pure EVA, which effectively improves the process fluidity of EVA/Al_2O_3 nanocomposites.

Table 1. The rheological indices of EVA/Al_2O_3 nanocomposite melts

Content of Al_2O_3	0	0.5%	1%	1.5%	2%	3%
Rheological index	0.56	0.47	0.47	0.47	0.49	0.48

Conclusions

Ethylene-vinyl acetate (EVA)/Al_2O_3 nanocomposites were prepared by means of a "one-pot" process. Al_2O_3 nanoparticles with a size of about 20 nm are homogeneously dispersed in the EVA matrix, and linked with EVA through chemical bonds. EVA/Al_2O_3 nanocomposites transform from brittleness to toughness when fractured. The mechanical properties of EVA/Al_2O_3 nanocomposites are superior to that of the pure EVA. The tensile strength and elongation at fracture of EVA/Al_2O_3 nanocomposite material with 1.5% Al_2O_3 fillers increase by 25.4% and 12.1%, respectively. The apparent viscosity of EVA/Al_2O_3 nanocomposite melts is lower than that of pure EVA, which effectively improves the process fluidity of EVA/Al_2O_3 nanocomposites.

Acknowledgements

Financial support from National 863 Project of China (grant number: 2003AA302310) is gratefully acknowledged.

References

1. G.R. Goward, F. Leroux, and L.F. Nazar, Electrochimica Acta 43 (1998) 1307-1313.
2. P.C. LeBaron, Z. Wang, and T.J. Pinnavaia, Applied Clay Science 15 (1999) 11-29.
3. D.J. Suh, Y.T. Lim, and O.O. Park, Polymer 41 (2000) 8557-8563.
4. X. Kornmann, H. Lindberg, and L.A. Berglund, Polymer 42 (2001) 1303-1310
5. M. Alexandre, G. Beyer, C. Henrist, R. Cloots, A. Rulmont, R. Jerome, and P. Dubois, Chemistry of Materials 13 (2001)

3830-3832.
6. A. Riva, M. Zanetti, M. Braglia, G. Camino, and L. Falqui, Polymer Degradation and Stability 77 (2002) 299-304.
7. H. Cai, F.Y. Yan, Q.J. Xue, and W.M. Liu, Polymer testing 22 (2003) 875-882.
8. P. Meneghetti, S. Qutubuddin, and A. Webber, Electrochimica Acta 49 (2004) 4923-4931.
9. F. Croce, GB. Appetecchi, L. Persi, and B. Scrosati, Nature 394 (1998) 456-458.
10. A.B.R. Mayer, Materials Science and Engineering: C 6 (1998) 155-166.
11. G.B. Appetecchi, P. Romagnoli, and B. Scrosati, Electrochemistry Communications 3 (2001) 281-284.
12. A.S. Best, J. Adebahr, P. Jacobsson, D.R. MacFarlane, and M. Forsyth, Macromolecules 34 (2001) 4549-4555.
13. S.H. Chung, Y. Wang, L. Persi, F. Croce, S.G. Greenbaum, B. Scrosati and E. Plichta, Journal of Power Sources 97-98 (2001) 644-648.
14. P.A.R.D. Jayathilaka, M.A.K.L. Dissanayake, I. Albinsson, and B.-E. Mellander, Electrochimica Acta 47 (2002) 3257-3268.
15. M. Sternizke, M. Knechtel, M. Hoffman, E. Broszeit, and J. Rodel, J. Am. Ceram. Soc. 79 (1996) 121-128.
16. Y. Tang, Y. Hu, S.F. Wang, Z. Gui, Z.Y. Chen, and W.C. Fan, Polymer Degradation and Stability 78 (2002) 555-559.
17. L.Z. Qiu, R.C. Xie, P. Ding, and B.J. Qu, Composite Structures 62 (2003) 391-395.
18. L.Z. Qiu, J.P. Lv, and R.C. Xie, Chinese Journal of Semiconductors 24 (2003) 81-84.
19. Y. Tian, H. Yu, and S.S. Wu, Acta Polymerica Sinica 1 (2004) 129-131.